Journal of Applied Polymer Science

Curing behavior and network formation of cyanate ester resin/polyethylene glycol

Junxian Ma,[1,2] Xuefeng Lei,[2] Di Tian,[1] Liangjie Yuan,[1] Chongshan Liao[2]

[1]College of Chemistry and Molecular Sciences, Wuhan University, Wuchang District of Wuhan City, Luojiashan Road Number 16, Wuhan 430072, People's Republic of China

[2]Department of Chemistry and Biology, University of Electronic Science and Technology of China, Zhongshan Institute, Zhongshan 528402, China

Correspondence to: L. Yuan (E-mail: mjxld@163.com)

ABSTRACT: The mechanism and kinetics of the curing reaction of cyanate ester (CE) resin modified with polyethylene glycol were investigated by means of differential scanning calorimetry (DSC) and Fourier-transform infrared spectroscopy (FTIR). The relationship of heat flow versus conversion rate was used to evaluate the effects of polyethylene glycol (PEG) on the curing reaction of CE. DSC results showed that the addition of PEG decreased the curing temperature of CE effectively when its content was less than 20 wt %. The curing behavior of CE/PEG still complies with the self-catalytic kinetic model proposed by Kamal. The effects of PEG content on the kinetics parameters and conversion rate of the curing reaction were discussed. FTIR results indicated that the –OH groups in PEG participated in the polymeric reaction of CE and formed –O–C (=NH) –O– structure through block copolymerization, which extended the chain length between triazine rings and reduced the density of triazine rings. © 2014 Wiley Periodicals, Inc. J. Appl. Polym. Sci. **2015**, *132*, 41841.

KEYWORDS: cross-linking; differential scanning calorimetry (DSC); kinetics; thermosets

Received 25 June 2014; accepted 6 December 2014
DOI: 10.1002/app.41841

INTRODUCTION

Cyanate ester (CE) resins are currently used widespread in structural aerospace composites and electronic insulation as matrix resin for their excellent mechanical properties, high thermal stability, radiation and flame resistance, low outgassing, and minimal water absorption.[1–4] However, the applications of CE are restricted by high curing temperature required and low impact resistance originated from their high cross-link density. Therefore, it shows the importance to manufacture the reinforcement and lower curing temperature of CE resins for high-performance applications in particular.

Now, the methods of toughening modification of CE resins are shown as follows:[4,5] (1) Copolymerization with thermosetting resin.[6] (2) Blending with thermoplastic resins, such as polysulfone,[7,8] polyarylate,[9] poly (etherimide)[10] and so on. (3) Application of reactive elastomers, for instance, thermoplastic resin and rubber with active functional groups.[11–13] (4) Block copolymerization with polyhydric alcohol, including polyether or polyester polyol.[14–16] The main aim of the above modifications is to control the molecular structure or morphological structure, which is necessary to achieve significant toughening. At the same time, the addition of modifiers would influence the curing temperature and performance of CE resins. Therefore, it is very important to research the curing behavior of modified CE resins.

The curing mechanism of pure CE resin belongs to self-catalyzed reaction process and incorporates two stages. First, –OCN groups of cyanate monomers trimerize to form a trimer, namely triazine. Second, the trimers copolymerize to form polycyanurates containing triazine ring by the catalysis of the hydroxy functional groups in the CE monomer.[17–19]

Compared with pure CE resin, the mechanism and the curing kinetics parameters of modified CE resins have been altered on account of the participation of modifying agent in the curing reaction. So far, the curing behaviors of modified CE resins by copolymerizing additives, such as epoxy resin (EP), bismaleimide (BMI), aromatic polyesters, amorphous thermoplastics, liquid rubber, have been studied by the methods of differential scanning calorimetry (DSC) and Fourier-transform infrared spectroscopy (FTIR).[20–25] However, the influence of dihydric alcohol modifier on the curing dynamics of CE resin is rarely reported.

In this study, we propose that polyethylene glycol (PEG, $M_n = 600$) could be used as modifiers to toughen CE resins. The hydroxyl groups in PEG copolymerize with –OCN

Table I. DSC Results of the CE/PEG in Nitrogen Atmosphere (50 mL min^{-1}) with Heating Rate of 5°C min^{-1}

Samples	Onset temperature (°C)	Peak temperature (°C)	End temperature (°C)	Duration (min)	ΔH_T (Jg^{-1})
Pure CE	175	245.83	297	24.4	157.46
CE/20 wt % PEG	97	168.67	224	25.4	62.80
CE/20 wt % PEG/0.02 wt % DBTDL	120	161.17	209	19.5	92.86
CE/20 wt % PEG/0.05 wt % DBTDL	83	158.83	219	27.2	139.35
CE/20 wt % PEG/0.1 wt % DBTDL	67	144.33	230	32.6	245.15
CE/10 wt % PEG/0.05 wt % DBTDL	90	191	244	30.8	264.20
CE/30 wt % PEG/0.05 wt % DBTDL	77	170.5	248	34.2	71.62

functional groups in cyanate monomers to form block copolymers, which could effectively reduce the cross-link density of triazine rings and improve the chain structure flexibility. Here, we investigated the influences of PEG and dibutyltin dilaurate catalyst on the curing behavior of CE resins by the methods of DSC and FTIR and explored the curing dynamics mechanism of CE resins containing PEG.

EXPERIMENTAL

Materials

CE (2,2-Bis-(4-cyanatophenyl) propane, melting point: 79°C) was supplied by Special Structure Institute of China Aero-Industry (Jinan, China). Polyethylene glycol (PEG, $M_n = 600$) was provided by Guang Dong Guanghua Sci-Tech Co., Ltd.

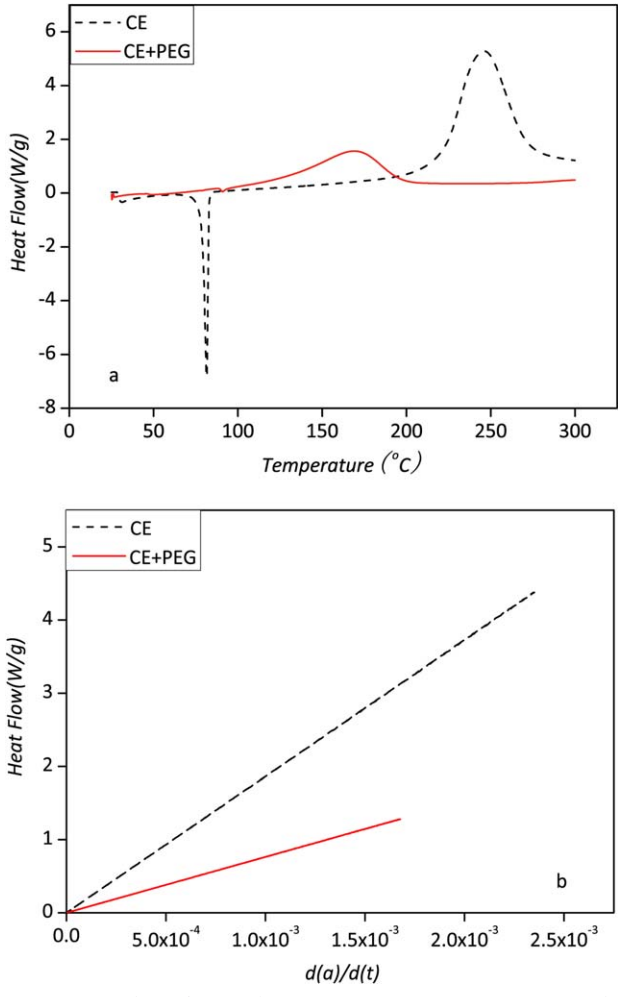

Figure 1. DSC plots of CE and CE/20 wt % PEG in nitrogen atmosphere (50 mL min^{-1}.) with a heating rate of 5°C min^{-1}. (a) Dynamic scanning curves of DSC, (b) Heat flow versus $d\alpha/dt$. [Color figure can be viewed in the online issue, which is available at wileyonlinelibrary.com.]

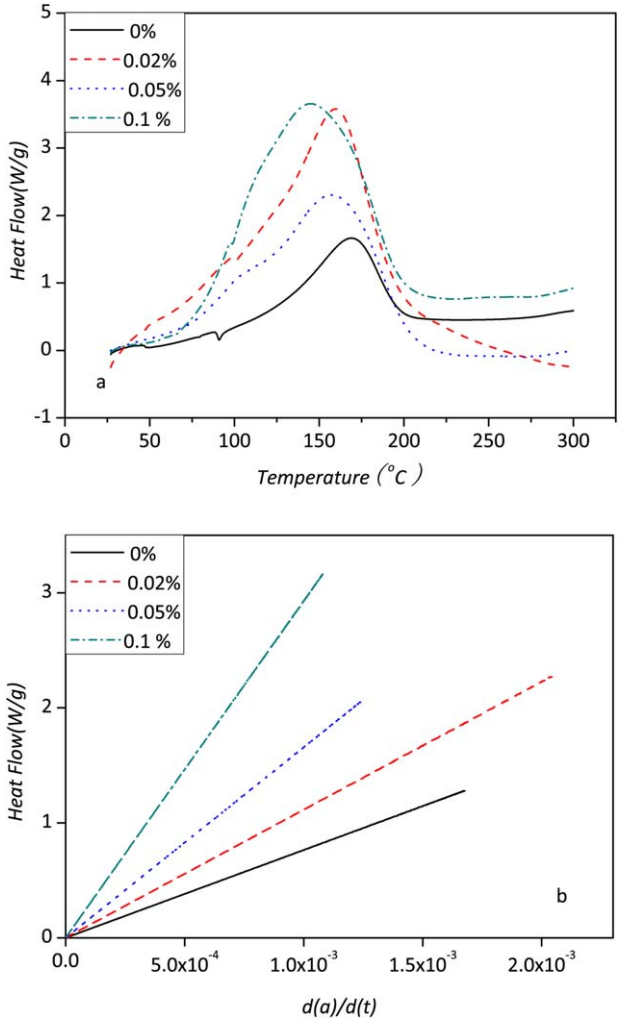

Figure 2. DSC plots of CE/PEG with different catalyst content in nitrogen atmosphere (50 mL min^{-1}) with a heating rate of 5°C min^{-1}, (a) Dynamic scanning curve of DSC, (b) Heat flows versus $d\alpha/dt$. [Color figure can be viewed in the online issue, which is available at wileyonlinelibrary.com.]

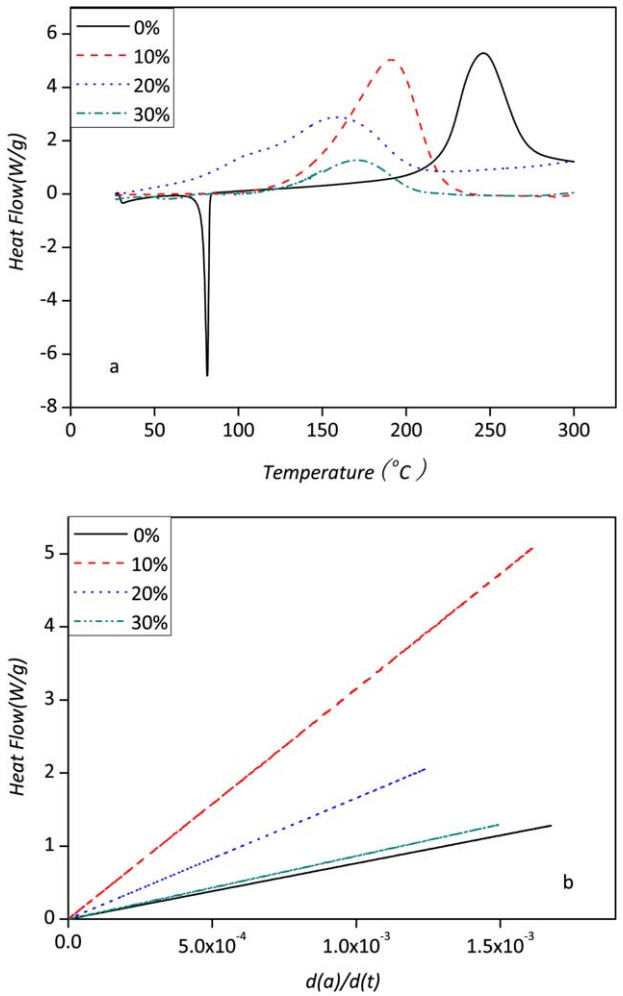

Figure 3. DSC plots of CE/PEG in nitrogen atmosphere (50 mL min^{-1}.) with a heating rate of 5°C min^{-1}, (a) Dynamic scanning curves of DSC for different content of PEG, (b) Heat flow versus $d\alpha/dt$ for different content of PEG. [Color figure can be viewed in the online issue, which is available at wileyonlinelibrary.com.]

Dibutyltin dilaurate (DBTDL, TCI) was purchased from Sinopharm Chemical Reagent Co., Ltd.

Preparation of CE/PEG/DBTDL

In this study, the mixtures of CE/PEG/DBTDL were designated by the weight ratio of their components in this order: CE, PEG, and DBTDL. For instance, 100 wt % CE and 10 wt % PEG was abbreviated as CE/PEG = 100/10. Similarly, a ternary blend containing 100 wt % CE, 10 wt % PEG, and 0.05 wt % DBTDL was coded asCE/CTBN/DBTDL = 100/10/0.05. The blends were prepared as follows: CE was firstly placed in a three-neck round-bottomed flask with a mechanical stirring at 90°C till a clear liquid was obtained. Then, according to compound design, the preweighted PEG and DBTDL, respectively, were added into flask with continuous stirring. The mixture was maintained for 10 min to obtain uniform and transparent solution. Finally, the solution was diluted with acetone and sealed in glass bottles and stored at −5°C for further use.

Characterizations

Differential scanning calorimetry (DSC) measurements were made on a model Q100 DSC (TA instruments, Inc.) for isothermal and dynamic cure experiments. A helium flow of 50 mL min^{-1}. was used as purge gas for all the DSC experiments. The samples were transferred into hermetic aluminum pans using a pipette and placed in 40°C oven for 10 min to volatilize acetone completely. On the one hand, the samples were put into DSC cell to be tested in the dynamic mode from room temperature to 300°C at the heating rate of 5°C min^{-1}. The results were used to evaluate the dynamic behavior of the samples in whole process of heating. On the other hand, the samples in DSC cell were isothermally cured from 1 to 4 h on the specified curing temperature at the rapid heat rate of 100°C min^{-1}. The resulted isothermal scans were used to discuss the isothermal curing behavior of the mixtures.

FTIR measurements were performed with a Nicolet 380 FTIR Spectrometer, using 64 scans with a 2 cm^{-1} resolution step. The blend solution diluted with acetone was dropped onto the KBr matrix and placed in oven at 40°C for five min until the acetone was volatilized completely. Then, the samples without acetone were cured for some time at different temperatures and scanned to obtain the IR spectra in the range of 400–4000 cm^{-1}.

Theory

For the thermoset, the curing dynamic behavior can be described with thermodynamic parameters.[26] Here, the conversion of curing reaction at time t can be defined as follows:

$$\alpha_t = \frac{\Delta H_t}{\Delta H_T} \tag{1}$$

Where, α is the conversion of curing at time t, H_t is the reaction heat at time t, and ΔH_T is the total reaction heat shown on a typical nonisothermal experiment. In this experiment, the ΔH_T was determined by scanning of uncured samples with a heating rate of 5°C min^{-1}, as shown in Table I.

Correspondingly, the conversion rate of curing reaction at time t can be defined as follows:

$$\frac{d\alpha}{dt} = \frac{d\Delta H_T/dt}{\Delta H_T} \tag{2}$$

Where, $d\alpha/dt$ is the conversion rate at time t.

The dynamic scanning DSC curve of the curing reaction for pure CE and CE/PEG/DBTDL have been simulated according to the self-catalytic kinetic model proposed by Kamal (1974),[27] which is shown in Figure 4. Here, the empirical rate equation is expressed as follows:

$$\frac{d\alpha}{dt} = (k_1 + k_2\alpha^m)(1-\alpha)^n = k(1-\alpha)^n \tag{3}$$

Where, k_1 and k_2 are the rate constants, m and n are the reaction orders, and k is the kinetic rate constant under chemically controlled condition. The temperature dependence of any rate constant is given by the Arrhenius relationship as follows:

$$\mathrm{k} = \mathrm{A}\exp\left(-\frac{E_\alpha}{\mathrm{RT}}\right) \tag{4}$$

Where, E_α is the activation energy, R is the gas constant, T is absolute temperature, and A is the pre-exponential factor.

Based on the data provided by the isothermal scanning DSC curves and the corresponding $d\alpha/dt$ versus α figures of the pure

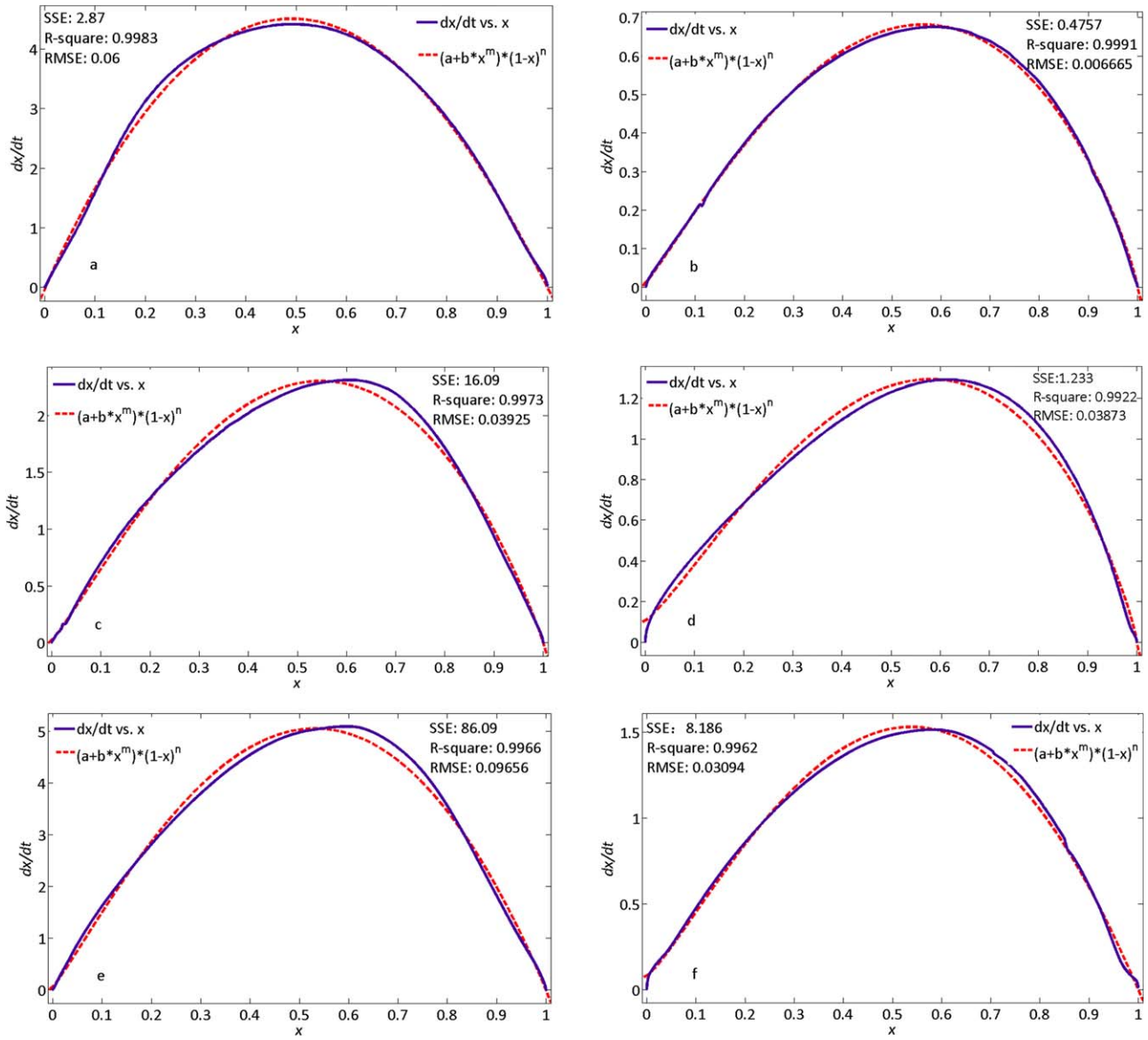

Figure 4. Simulation for the dynamic scanning DSC curve of pure CE and CE/PEG/DBTDL resins in nitrogen atmosphere (50 mL min^{-1}) with a heating rate of 5°C min^{-1}, (a) pure CE, (b) CE/5 wt % PEG/0.05 wt % DBTDL, (c) CE/10 wt % PEG/0.05 wt % DBTDL, (d) CE/20 wt % PEG/0.05 wt % DBTDL, (e) CE/30 wt % PEG/0.05 wt % DBTDL, (f) CE/50 wt % PEG/0.05 wt % DBTDL. [Color figure can be viewed in the online issue, which is available at wileyonlinelibrary.com.]

and modified CE resins at different isothermal temperatures, the curing reaction kinetics constants E_α, k, n, and A can be obtained according to eqs. (3) and (4).

RESULTS AND DISCUSSION

Dynamic Scanning Analysis

Figure 1 shows the nonisothermal DSC plots of CE and CE/20 wt % PEG in nitrogen atmosphere (50 mL min^{-1}) with a heating rate of 5°C min^{-1}. The addition of PEG obviously altered the curing exothermic temperature of CE. Compared with pure CE, the onset curing temperature of CE/20 wt % PEG significantly decreased by 78°C, and the exothermic peak temperature reduced from 245.83°C to 168.67°C. The plot of heat flow versus $d\alpha/dt$ showed that the addition of PEG decreased the maximum curing conversion rate and the heat flow value. The result indicated that the PEG participated in the curing reaction of CE, which hindered the cyclotrimerization of CE and then resulted in the lower curing conversion rate and heat flow.

Figure 2 shows the effects of catalyst (DBTDL) on the dynamic curing process of CE/PEG resin. The exothermic peak temperature decreased, while the heat flow increased with increasing DBTDL content. At the same time, the maximum conversation rate of ternary mixture reduced as compared with that of binary mixture without catalyst, except for the ternary mixture with 0.02 wt % DBTDL. The curing reactions of CE/PEG systems are complicated, mainly including the cyclotrimerization of CE and the block copolymerization between PEG and CE monomers. The results of Figure 2 indicated that the addition of DBTDL could catalyze both reactions mentioned previously.

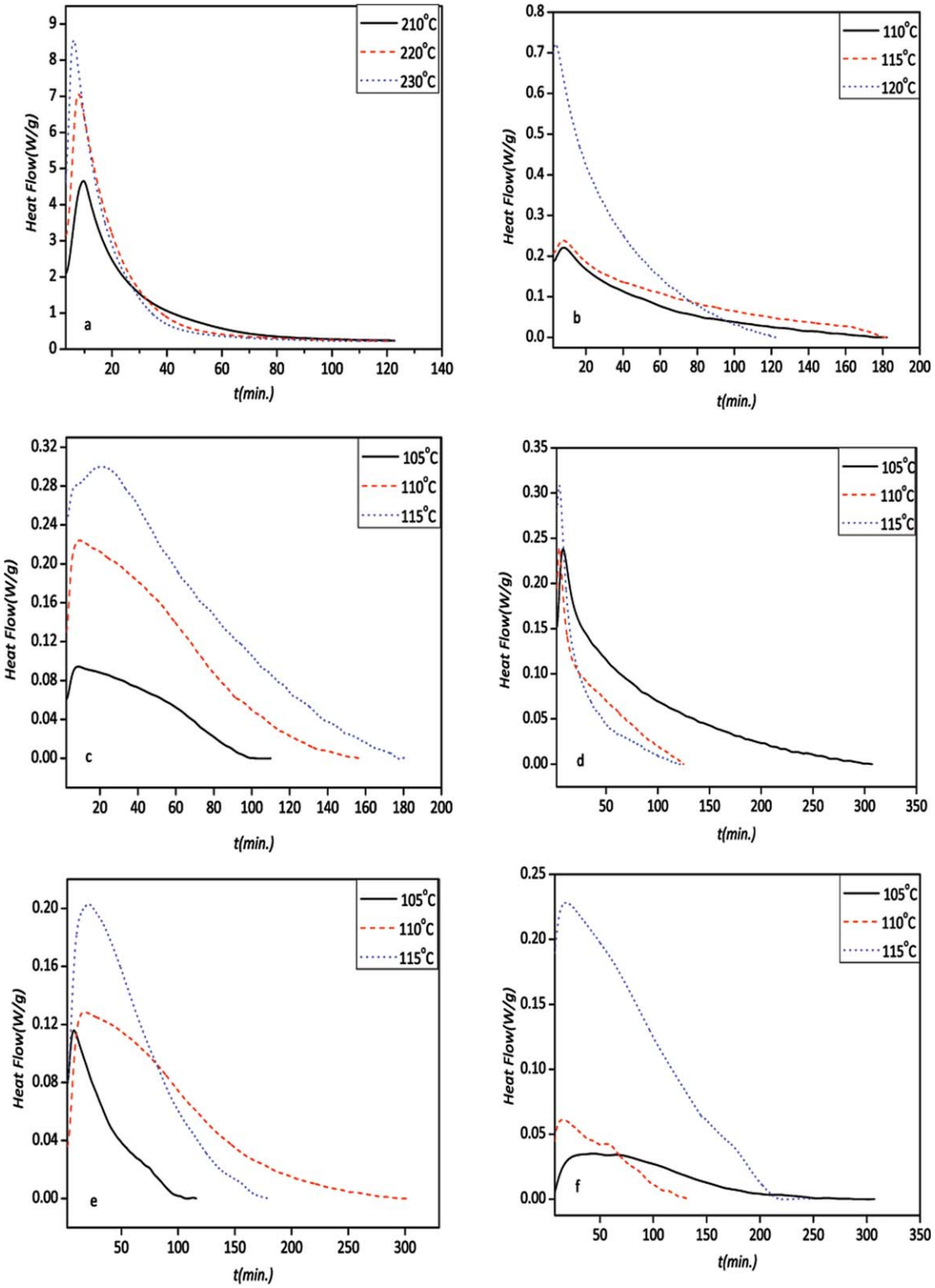

Figure 5. Isothermal scanning DSC curves for CE/PEG/DBTDL at different isothermal curing temperature, (a) pure CE, (b) CE/5 wt % PEG/0.05 wt % DBTDL, (c) CE/10 wt % PEG/0.05 wt % DBTDL, (d) CE/20 wt % PEG/0.05 wt % DBTDL, (e) CE/30 wt % PEG/0.05 wt % DBTDL, (f) CE/50 wt % PEG/0.05 wt % DBTDL. [Color figure can be viewed in the online issue, which is available at wileyonlinelibrary.com.]

Figure 3 demonstrates the effects of PEG content on the dynamic curing process of CE/0.05 wt % DBTDL. The onset and peak temperature dramatically decreased with increasing PEG content, up to 20 wt %. However, when the PEG content arrived to 30 wt %, the onset and peak temperature increased. The plot of heat flow versus $d\alpha/dt$ revealed that the heat flows

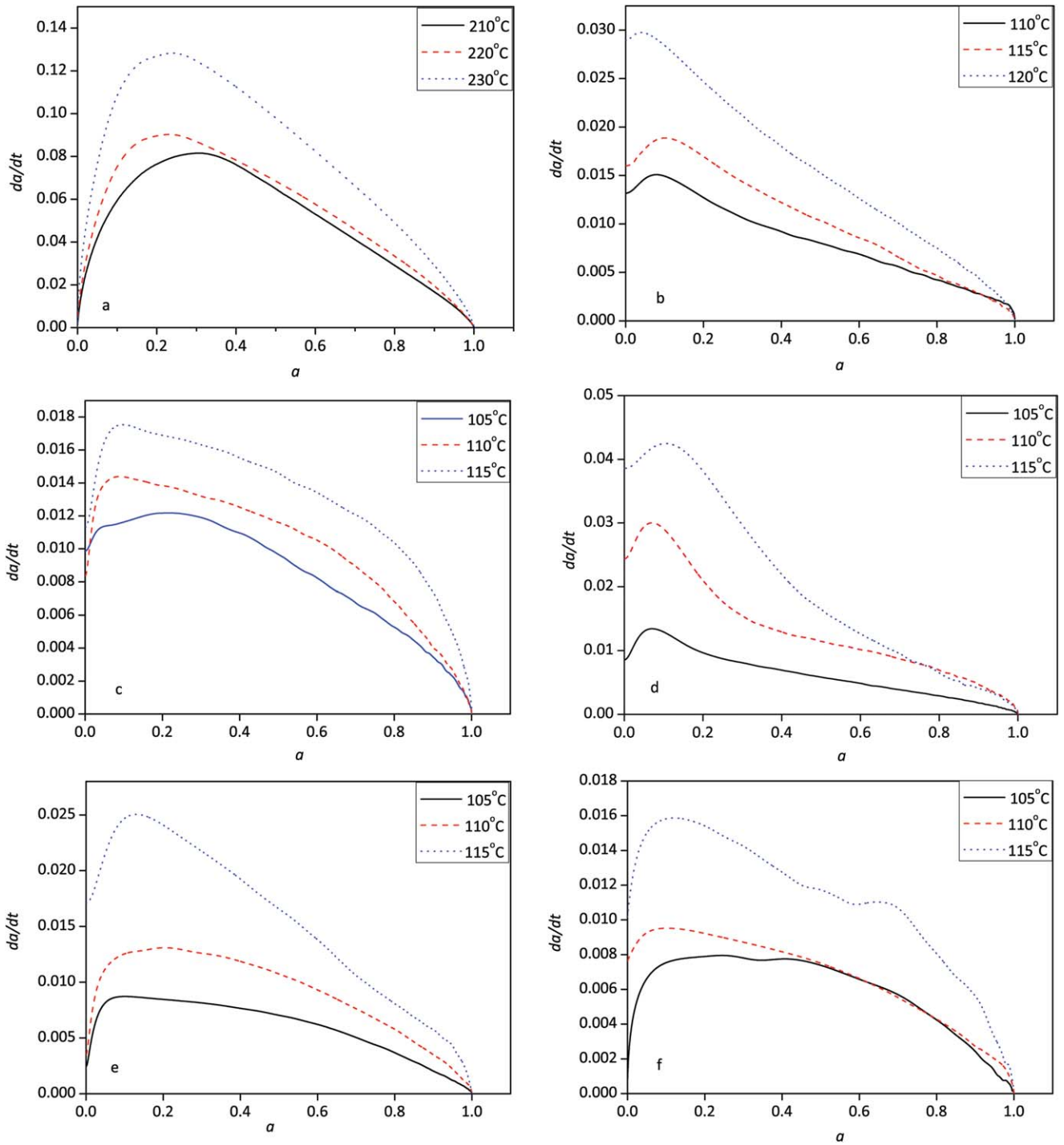

Figure 6. $d\alpha/dt$ versus α for CE/PEG/DBTDL at different isothermal curing temperature, (a) pure CE, (b) CE/5 wt % PEG/0.05 wt % DBTDL, (c) CE/10 wt % PEG/0.05 wt % DBTDL, (d) CE/20 wt % PEG/0.05 wt % DBTDL, (e) CE/30 wt % PEG/0.05 wt % DBTDL, (f) CE/50 wt % PEG/0.05 wt % DBTDL. [Color figure can be viewed in the online issue, which is available at wileyonlinelibrary.com.]

of mixtures reduced with the increase in PEG content, but all the values were larger than that of pure CE. It can also be observed that the maximum conversion rates of mixtures are lower than that of pure CE. The DSC results of above-mentioned systems were all listed in Table I.

The above results of dynamic DSC scanning indicated that the incorporation of PEG and DBTDL can not only reduced the onset and peak temperature but also influenced the heat flow and conversation rate of the CE curing reaction. Compared with the CE system without PEG, the present of PEG evidently reduced the maximum conversation rate of curing reaction, which may be explained as following. The density of triazine rings formed by CE monomers decreased in the curing reaction because of the block copolymerization reacted between –OH

Table II. The Calculated Results of Chemical Reaction Kinetics Constant at Different Curing Temperature

PEG (wt %)	Temperature (°C)	k_1 ($\times 10^{-4}\cdot s^{-1}$)	K_2 ($\times 10^{-4}\cdot s^{-1}$)	m	n	$\ln A_1$	$\ln A_2$	E_1(kJmol^{-1})	E_2(kJmol^{-1})
0	210	33.67	876.7	0.3622	1.326	11.18	15.01	67.62	70.04
	220	51.88	1049	0.4301	1.383				
	230	65.29	1133	0.2579	1.277				
5	110	0.8737	0.6781	1.459	0.3822	10.16	10.77	62.11	64.86
	115	1.123	0.8815	1.261	0.4724				
	120	1.144	1.138	0.9419	0.5553				
10	105	4.215	3.024	0.4198	0.8036	8.17	9.27	50.10	54.60
	110	5.190	3.794	0.2504	0.7143				
	115	6.356	4.733	0.1929	0.6878				
20	105	6.453	2.676	0.3685	0.7577	6.48	12.74	43.45	65.89
	110	7.730	3.518	0.1882	0.5890				
	115	9.216	4.593	0.3078	0.6932				
30	105	2.175	2.294	0.8837	0.8504	8.53	15.31	53.31	74.45
	110	2.714	3.126	0.7292	1.107				
	115	3.368	4.225	0.3969	0.9674				
50	105	0.6643	1.189	0.6257	0.8793	9.61	16.13	60.43	77.64
	110	0.8538	2.606	0.6205	0.5729				
	115	1.090	3.568	0.3806	0.8337				

groups in PEG and –OCN groups in CE, thus hindered the formation of the cross-linked networks and resulted in the decrease of the conversion rate of the whole curing reaction.

Isothermal Scanning Analysis

Figure 4 provides the simulation results of the dynamic scanning DSC curves for pure CE and a series of CE/PEG/0.05 wt % DBTDL resins with different contents of PEG in nitrogen atmosphere (50 mL min^{-1}) with a heating rate of 5°C min^{-1}. The results perfectly indicated that the curing process of CE/PEG/DBTDL still comply with the self-catalytic kinetic model proposed by Kamal.

Figure 5 shows the isothermal scanning DSC curves of heat flow versus time for the CE/PEG/ DBTDL system at different isothermal curing temperature. The plots of $d\alpha/dt$ versus α for the CE/PEG/DBTDL blend are shown in Figure 6. All blends have low conversion rates at the beginning of the reaction, and then, the conversion rate increased and shown a maximal value with curing process, which is in accordance with the typical self-catalytic behavior. In Figure 6(a), the conversion of pure CE at the maximal conversion rate appeared at about 0.2, while for the CE/PEG/DBTDL systems, the conversions were all less than 0.2 significantly, indicating that the block copolymerization of PEG and CE reduced the conversion of cyclotrimerization. Table II provides the calculated results of chemical reaction kinetics constant at different curing temperature, according to the autocatalytic model (eq. (3)) and the Arrhenius relationship (eq. (4)).

The curing process of CE/PEG/DBTDL maybe includes the following reactions. (1) The cyclotrimerization of CE and the further network formation by cyclotrimerization. (2) The block copolymerization reaction between –OH groups in PEG and –OCN groups in CE monomers or trimers. (3) The formation of small molecule chains and other byproducts reacted between PEG (or other active hydrogen) and CE. Figure 7 shows the effects of PEG content on the activation energy and the pre-exponential factor. Here, the kinetic parameters k_1, E_1, and lnA_1 represented the effects of PEG in some reactions at the initial stage of the curing process, such as the formation of block structures, trimers, and small molecule chains. The addition of PEG diluted the aggregation of CE monomers and thus reduced the collision frequency of –OCN groups, leading to a lower conversation rate of CE trimers as compared with that of pure CE. But the block copolymerization reaction was accelerated with the increasing PEG content due to the increased collision frequency between –OH groups and –OCN groups. Besides, the intermediates formed in the reaction of –OH with –OCN possibly have catalytic influence on the cyclotrimerization of CE. Based on the above-mentioned reactions, k_1 increased, while E_1 and lnA_1 decreased with the increasing of PEG. However, when the content of PEG was up to 20%, k_1 decreased, while E_1 and lnA_1 increased, since the continued decreasing of –OCN resulted in the significant decline of conversion rate constant ofCE trimers.

K_2, E_2, and lnA_2 revealed the influence of PEG in the cross-linking reaction at the later stage of the curing process. In this process, the formation of cross-linked network belonged to diffusion controlled for the effects of steric hindrance and the obstructing effect among large molecules. Compared with pure CE, the participation of PEG not only reduced the collision of –OCN groups but hindered the intermolecular interaction among trimers, making the collision frequency and orientation factor

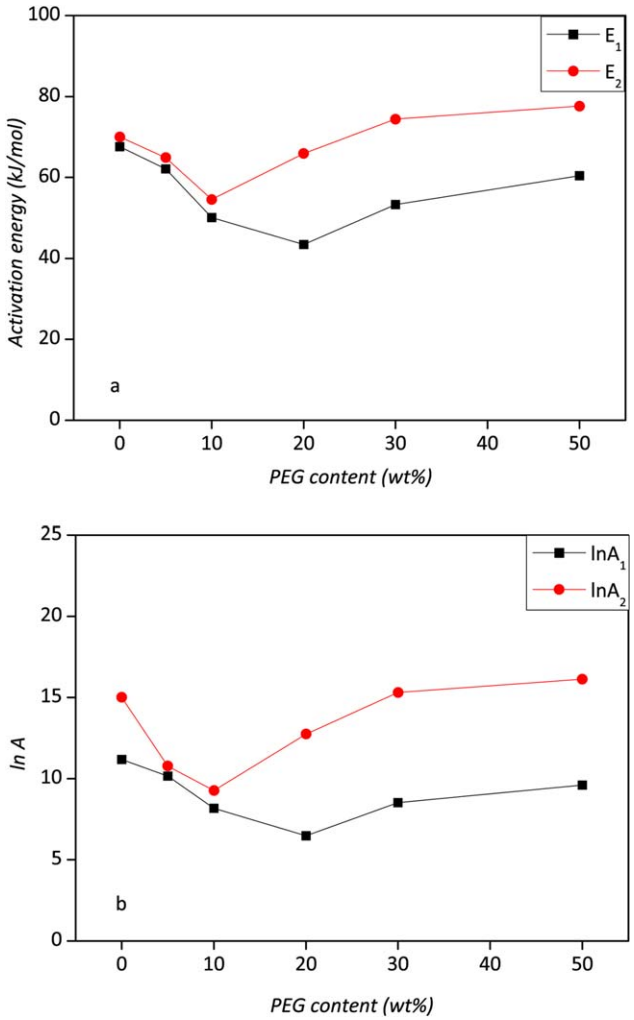

Figure 7. Activation energy (a) and pre-exponential factor (b) versus PEG content. [Color figure can be viewed in the online issue, which is available at wileyonlinelibrary.com.]

Table III. Characteristic Infrared Spectra Absorptions for Possible Structure

Wave number (cm^{-1})	Absorbing group	Group from compound
1076	Either in -C-O-C-	Polyethylene glycol
2875, 2970	-CH2-	
3364	-OH	
1197, 1167	Either in Ar-O-C-	2,2-Bis-(4-Cyanatophenyl) propane
1503	-CH3	
2236, 2270	-C≡N	
3062	-CH in aryl group	
1564	Triazine	Aryl cyanurate
1365	-O-	
	either in -N= C-O-Ar	Oxazoline
1679	-N=C-O-	
	-O-C(=NH)-O-	Imidocarbonate
1718	C=O	Isocyanurate

of the curing reaction decreased, thus leading to a lower rate constant. On the other hand, PEG played plasticizing role at a certain degree in the curing reaction, which enhanced the diffusion ability of trimers in the mixture system. When the PEG content was less than 10 wt %, k_2 increased, while E_2 and lnA_2 decreased with the increasing of PEG. But when the PEG content was more than 10 wt %, the plasticizing effect was no longer significant. At the same time, the steric hindrance increased with the increasing intermediates, which resulted the decrease in the collision frequency and orientation factor of the –OCN groups. Therefore, k_2 decreased while E_2 and lnA_2 increased with the increasing of PEG.

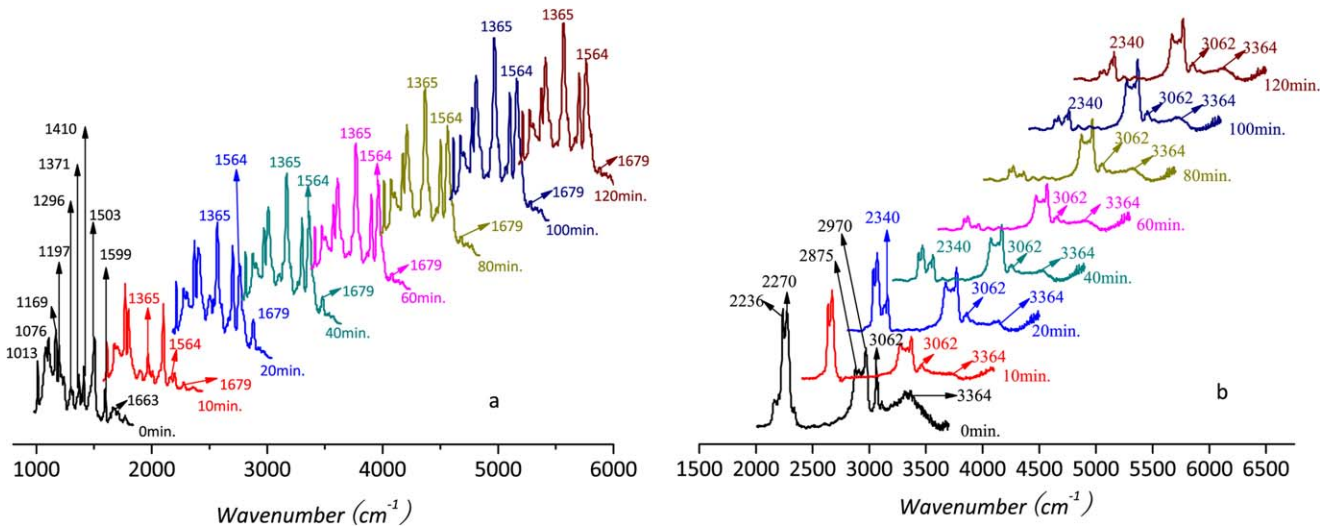

Figure 8. FTIR spectra of CE/20 wt % PEG/0.05 wt % DBTDL with time cured at 120°C (a) in the range of 1000 cm^{-1} and 2000 cm^{-1}, (b) in the range of 2000 cm^{-1} and 3800 cm^{-1}. The peak at 2340 cm^{-1} is the absorption bond of CO_2. [Color figure can be viewed in the online issue, which is available at wileyonlinelibrary.com.]

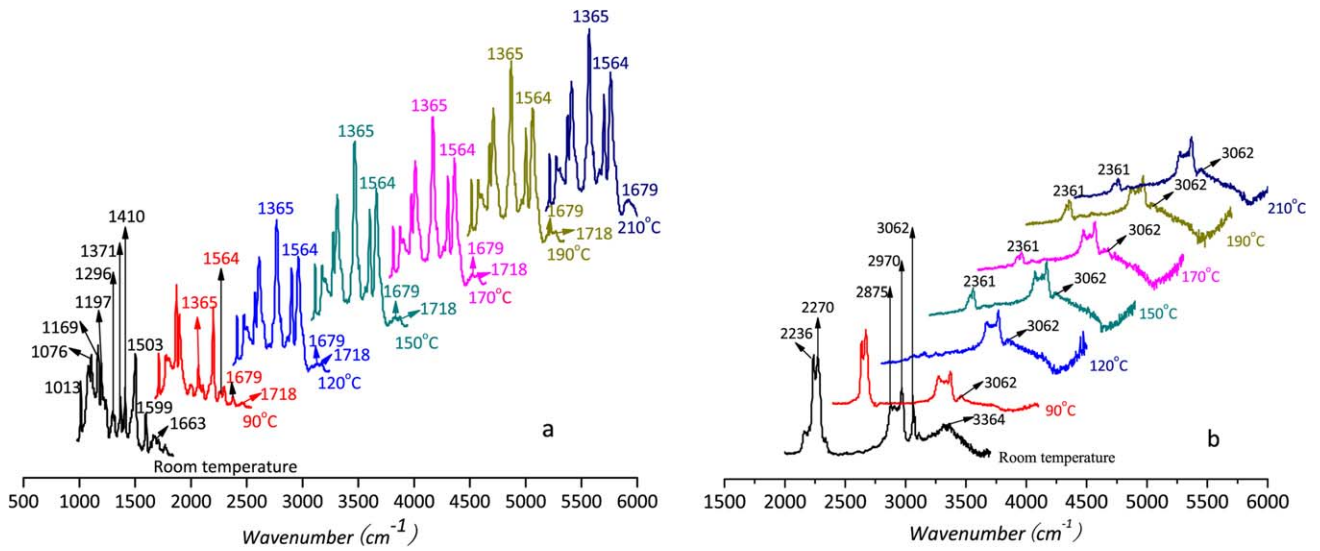

Figure 9. FTIR spectra of CE/20 wt % PEG/0.05 wt % DBTDL with temperature cured for 2 h (a) in the range of 1000 cm^{-1} and 2000 cm^{-1}, (b) in the range of 2000 cm^{-1} and 3800 cm^{-1}. The peak at 2360 cm^{-1} is due to the absorption bond of CO_2. [Color figure can be viewed in the online issue, which is available at wileyonlinelibrary.com.]

FTIR Analysis

Figure 8 gave the spectra evaluation of CE/20 wt % PEG/0.05 wt % DBTDL with different curing time at 120°C. Corresponding characteristic infrared spectra absorptions for possible structure were listed in Table III.

In Figure 8(a), the absorbing peaks representing the groups of triazine (aryl cyanurate) appeared at 1365 cm^{-1} and 1564 cm^{-1} after the curing reaction proceeding for 10 min. Furthermore, the bonds gradually increased with the curing time. The intensity of the peak –O–C(=NH)–O– located at 1679 cm^{-1} firstly

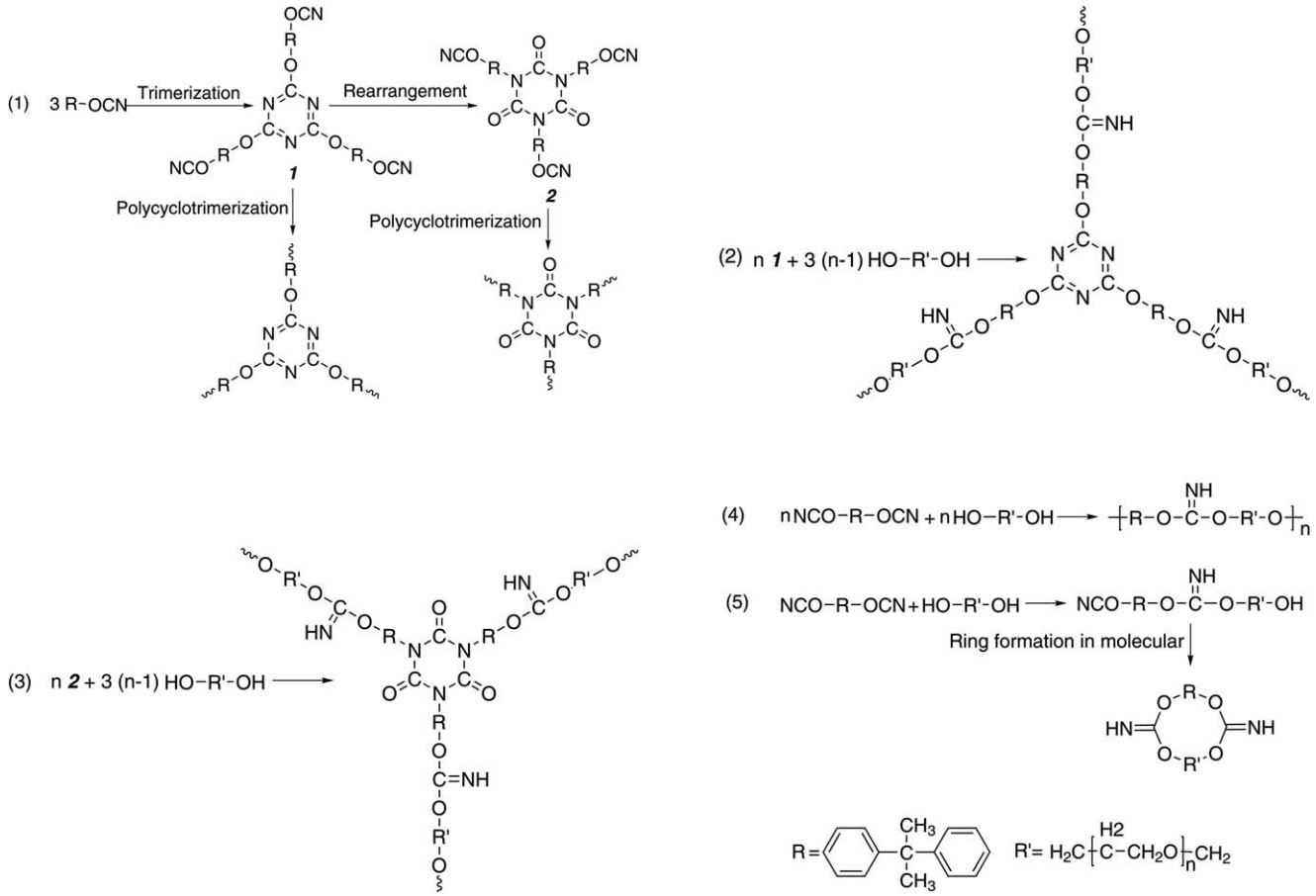

Scheme 1. Curing mechanism of CE resin modified by PEG.

increased and then decreased with the extending of curing time. In Figure 8(b), the characteristic absorption bond of the –C≡N functional group in CE monomers gradually decreased at 2236 cm^{-1} and 2270 cm^{-1} in the curing process. The intensity of absorption peak of –OH from PEG at 3364 cm^{-1} rapidly decreased at the beginning of curing process. The results indicated that the curing reaction of CE resins had occurred and formed triazine at 120°C and its content gradually increase with the increase in curing time. The intensity changes of peak –O–C(=NH)–O– at 1679 cm^{-1} maybe could illuminate the rearrangement of triazine ring.

The formation of triazine was the main reaction when the curing reaction started, so the intensity of the peak increased. While after 20 min., the triazine rearranged, the –C=N– bonds in triazine partially changed to –(C=O)– bonds and the intensity of the peak began to decreased until 60 min. At the same time, other reactions are present except the above curing reaction, including the formation of isourea or imidocarbonate for the reaction between –OCN functional group and –OH group from PEG. In addition, the absorption bond of –CH from aryl group at 3062 cm^{-1} in Figure 8(b) decreased when the curing reaction began. The reason was not clear only according to the result of infrared spectra.

Figure 9 shows FTIR spectra of CE/20 wt % PEG/0.05 wt % DBTDL with different cured temperature for 2 h. In Figure 9(a), the peaks at 1564 cm^{-1}, 1365 cm^{-1}, 1679 cm^{-1}, and 1718 cm^{-1} represented the absorbing bonds of triazine in aryl cyanurate, –O– in –N=C–O–Ar and oxazoline, –O–C(=NH) –O– in imidocarbonate, and C=O in isocyanurate, respectively. Among them, the intensity of the peaks at 1564 cm^{-1} and 1365 cm^{-1} were enhanced gradually with the increase in temperature, especially for the peak of 1365 cm^{-1}. The absorption peaks at 1679 cm^{-1} and 1718 cm^{-1} were gradually coupled together to form one absorption peak at 1679 cm^{-1} at 210°C. In Figure 9(b), the absorption bond of –C≡N at 2236 cm^{-1} and 2270 cm^{-1} almost disappeared when the curing temperature arrived to 120°C. The results manifested that the curing reaction of the CE/PEG/DBTDL mixtures not only included the self-polymerization reactions of triazine, but also possibly involved other reactions, such as the reaction between –OCN and –OH to form imidocarbonate structure, the formations of isocyanurate structure at low temperature and oxazoline structure at high temperature.

Curing Mechanism of CE/PEG Resins

In the curing process of CE/PEG/DBTDL, the mainly reactions were as follows: (1) –OCN functional groups in the CE monomers trimerized to form trimer and further copolymerized to form polycyanurates containing triazine ring. (2) PEG entered into the molecular network through reacting with the –NCO functional group of CE monomer to form embedded structure, possibly accompanied with some reactions including the formation of the straight chain structure through copolymerization between the –NCO in the CE monomers and the –OH in PEG, and the formation of the cyclic structure through the intramolecular reaction of the binary copolymer formed by the –NCO in the CE monomers and the -OH in PEG. The reactions were listed as follows. (Scheme 1)

CONCLUSION

The curing behavior of CE/PEG/DBTDL still complied with the self-catalytic kinetic model proposed by Kamal. The addition of PEG reduced the curing activation energy ($E\alpha$) distinctly, leading to the curing reaction beginning at lower temperature. However, it also decreased the heat flow and the conversion rate of the curing reaction for the present of PEG hindered the self-polymerization among the CE monomers to form triazine rings. Although the incorporation of catalysis enlarged the heat flow of curing reaction, it did not obviously accelerate the conversion rate, which disclosed that the catalysis mainly promoted the reactions between the –OH groups in PEG and –OCN groups in CE monomers. In the process of curing reaction, –OH and –OCN were polymerized to form –O–C (=NH) –O– groups, which extended the chain length between triazine rings and reduced the triazine ring density in the cross-linked network.

ACKNOWLEDGMENTS

This study was supported by grants from the National Nature Science Foundation of China (No. 21471119), Guangdong Province Ministry of Education Project on the Integration of Industry, Education and research (No. 2012B091100434) and Zhongshan Institute Scientific Research Initial Foundation (No. 2013A3FC0262).

REFERENCES

1. Simon, S. L.; Gillham, J. K. *J. Appl. Polym. Sci.* **1993**, *47*, 461.
2. Snow, A. W.; Buckley, L. J.; Armistead, J. P. *J. Polym. Sci. Part A: Polym. Chem.* **1999**, *37*, 135.
3. Hamerton, I. In Chemistry and Technology of Cyanate Ester Resins, Blackie Academic & Professional: New York, **1994**; p 357.
4. Hamerton, I.; Hay, J. N. *Polym. Int.* **1998**, *47*, 465.
5. Lu, S. H.; Zhou, Z. W.; Fang, L.; Liang, G. Z.; Wang, J. L. *J. Appl. Polym. Sci.* **2007**, *103*, 3150.
6. Nair, C. P. R.; Mathew, D.; Ninan, K. N. *Adv. Polym. Sci.* **2001**, *155*, 1.
7. Hwang, J. W.; Cho, K.; Yoon, T. H.; Park, C. E. *J. Appl. Polym. Sci.* **2000**, *77*, 921.
8. Woo, E. M.; Shimp, D. A.; Seferis, J. C. *Polymer* **1994**, *35*, 1658.
9. Lijima,T.; Kunimi, T.; Oyama, T.; Tomoi, M. *Polym. Int.* **2003**, *52*, 773.
10. Harismendy, I.; Rio, M. D.; Marieta, C.; Gavalda, J.; Gomez, C. M.; Mondragon, I. *J. Appl. Polym. Sci.* **2001**, *80*, 2759.
11. Auad, M. L.; Frontini, P. M.; Borrajo, J.; Aranguren, M. I. *Polymer* **2001**, *42*, 3723.
12. Shi, H. H.; Fang, Z. P.; Gu, A. J.; Tong, L. F.; Xu, Z. B. *J. Appl. Polym. Sci.* **2007**, *106*, 3098.

13. Zeng, M. F.; Sun, X. D.; Wang, Y.; Zhang, M. Z.; Shen, Y. M.; Wang, B. Y.; Qi, C. Z. *Polym. Advan. Technol.* **2008**, *19*, 1664.
14. Fainleib, A. M.; Grigoryeva, O. P.; Hourston, D. J. *Macromol. Symp.* **2001**, *164*, 429.
15. Fainleib, A. M.; Grigoryeva, O. P.; Hourston, D. J. *Int. J. Polym. Mater.* **2001**, *51*, 57.
16. Fainleib, A. M.; Grigoryeva, O. P.; Hourston, D. J. *Polymer* **2001**, *42*, 8361.
17. Fyfe, C. A.; Niu, J.; Rettig, S. J.; Burlinson, N. E.; Reidsema, C. M.; Wang, D. W.; Poliks, M. *Macromolecules* **1992**, *25*, 6289.
18. Georjon, O.; Galy, J.; Pascault, J. P. *J. Appl. Polym. Sci.* **1993**, *49*, 1441.
19. Simon, S. L.; Gillham, J. K. *J. Appl. Polym. Sci.* **1993**, *47*, 461.
20. Urszula, S.; Paweł, M. *J. Therm. Anal. Calorim.* **2012**, *109*, 73.
21. Sheng, X.; Akinc, M.; Kessler, M. R. *J. Therm. Anal. Calorim.* **2008**, *93*, 77.
22. Vinnik, R. M.; Roznyatovsky, V. A. *J. Therm. Anal. Calorim.* **2004**, *75*, 753.
23. Pradhan, S.; Brahmbhatt, P.; Sudha, J. D.; Unnikrishnan, J. *J. Therm. Anal. Calorim.* **2011**, *105*, 301.
24. Szeluga, U.; Kurzeja, L. H.; Galina, J. J. *Therm. Anal. Calorim.* **2008**, *92*, 813.
25. Szeluga, U.; Kurzeja, L.; Galina, H. *Polym. Bullet.* **2008**, *60*, 555.
26. Lin, Y.; Jin, J.; Song, M.; Shaw, S. J.; Stone, C. A. *Polymer* **2011**, *52*, 1716.
27. Kamal, M. R. *Polym. Eng. Sci.* **1974**, *14*, 231.